Superconducting quantum circuits & Intel Core i9-14900K processor core

Technical and math Nodes;
A simplified circuit includes three circuit loops that are connected on node 1. In the leftmost loop, a signal generator drives the system. The next loop with the capacitor Csph represents the spherical SC shell. C 0 and L are the effective capacitance and inductance of the SC island, respectively. The superconducting phase $\phi 2$ on the central superconductor (node 2) and $\phi 1$ on the sphere (node 1) are separated by a Josephson junction modeled with nonlinear inductance LJ and effective capacitance CJ. The right loop demonstrates a simple example of measurement, an rf-SQUID (light blue), although many possible variations of external low-noise readout exist to detect the change of $\phi 1$ in time.

Circuit phases-measures:
Phase difference across JJ $\Delta\phi$ in terms of time, solved from the Lagrangian equation of motion, when $\omega 0 \approx 8.5\text{GHz}$, $\alpha \approx 2 \times 10{-}15\text{Wb}$, $V0 = 1\mu\text{V}$, $\omega = 150\text{MHz}$.

A plot of potential energy for EL = 1GHz × h, EJ = 25GHz × h. Blue is the ground state for each well while red is the first excited state. Inter-well tunneling may occur, in which microwave photons may be emitted or absorbed.

Possible particle acceleration with powerful processors like i9 intel processor
c) A plot of potential energy for EL = 1GHz × h, EJ = 25GHz × h. Blue is the ground state for each well while red is the first excited state. Inter-well tunneling may occur, in which microwave photons may be emitted or absorbed.

Gates:

a) Gate fidelity Fx of single-qubit gate Ux(π) versus η and Em. Here, EJ = 2Ez . b). Fx versus Em at various η as is labeled in the plot. c). Fx versus η at various Em/Ez as is labeled in the plot. d). The gate fidelity FC of two-qubit gate UC versus η at various Ecc/2π~ as is labeled in the plot.
b) Eigenenergies of the four-level system at EJ1/2π~ = 8.9 GHz, EJ2/2π~ = 13.9 GHz, and Emx/2π~ = 4 GHz
c) δ (solid lines) and η (dashed lines) as functions of $\Delta 1$ for U/t = 1, 5, 8, 10 and gq = 120MHz×2π
d) (a) A 3D superconducting cavity with one end coupled to a mechanical oscillator. (b) Three wave mixing scheme when $\omega = 2\omega\ 0$. (c) Four wave mixing scheme when ω , $2\omega\ 0$

Figure 1.2: Integration path to relate flux in a junction and the phase difference along the junction. Current density in the bounding superconductors.

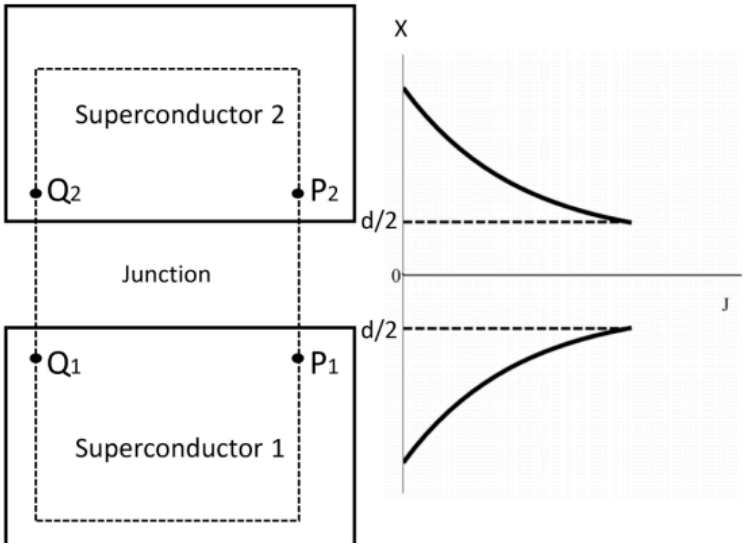

Consider two points on opposite sides of the barrier in a JJ as shown in Fig.1.2. If a gauge change is made so that $-\longrightarrow A\ 0 = -\longrightarrow A + \nabla\chi$ (1.22) where χ is an arbitrary scalar function, the phases at the two points become $\theta\ 0\ 1 = \theta 1 - (2e/\sim)\chi 1\ \theta\ 0\ 2 = \theta 2 - (2e/\sim)\chi 2$

In general, the critical current Ic depends on an applied magnetic field, as Eq.(1.32); in that case φ is the phase difference at the center of the junction if the junction characteristics are spatially uniform. The Josephson current relation reveals that Josephson junction includes a nonlinear inductance. This electron pair current is represented in the equivalent circuit model:

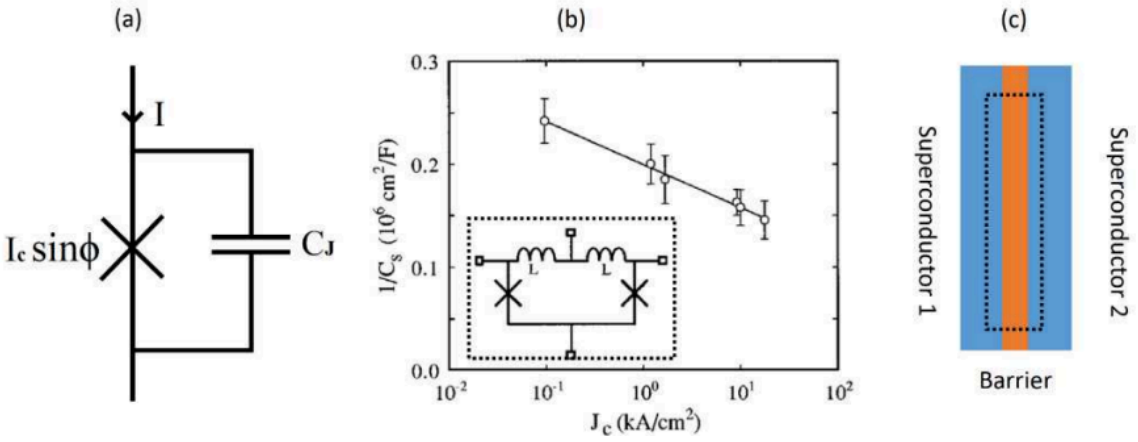

Figure 2.1: (a) Equivalent circuit model of a Josephson junction. Nonlinear inductor is connected parallelly with a capacitor. (b) Specific capacitance of Nb/AIOx/Nb Josephson junctions.

Formulas: The parallel-plane capacitance formula is assumed; C = ε0εrA/d where A is the junction area. Experimental evaluations have been published; a key result is shown in Fig.2.1(b), which gives the capacitance per unit area as a function of the Josephson current density for important niobium/aluminum oxide/niobium junctions.

Conductance: The conductance element G(V) in the equivalent circuit represents the quasiparticle current in the case of tunnel junctions. Its value is the slope of a line from the origin to the quasiparticle part of the I-V characteristic. In modeling of junctions for numerical computation, the conductance term is usually handled by piecewise-linear approximation. In some cases, analytic functions are fitted to the quasi-particle characteristic. Other Issues in Modeling: For junctions long enough that the inductance of the electrodes is significant with respect to the Josephson inductance LJ = Φ0/2πIc, as suggested in Fig.2.1(c), one should use a parallel set of circuits shown as two L 0 s in Fig.2.1(b)'s inset, connected by inductance representing the electrodes.

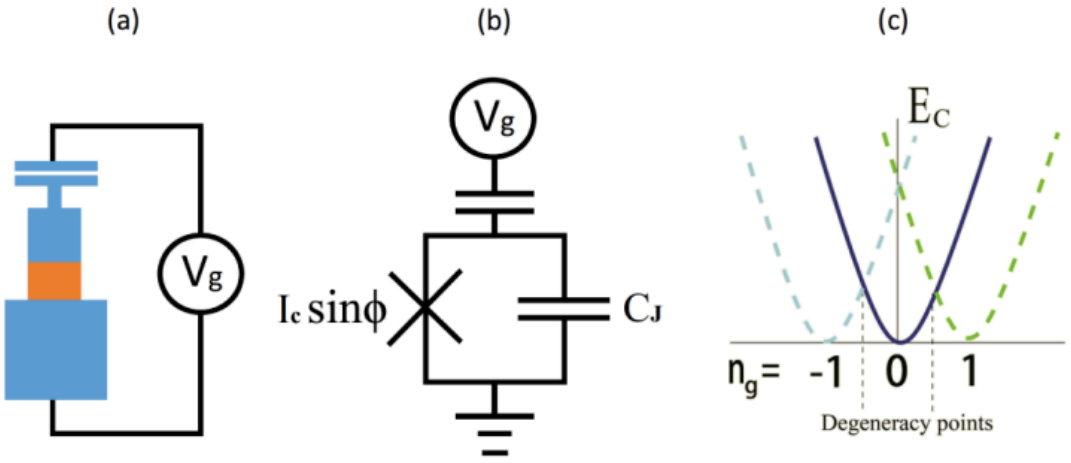

Figure 2.2: (a) A small superconducting island (small blue square) is connected to a big bulk of superconductor (blue) via a junction (Orange). Gate voltage Vg is used to bias the system energy. (b) Schematic circuit model of charge qubit. (c) Charge energy diagram.

We can see in the Hamiltonian (2.6) that phase difference φ behaves like position x in configuration space. So effective mass mE = ~ 2 2Ec , and canonical momentum p = ~ 2 · φ 2Ec . In quantum limit, the quadratures bφ and bp need to be quantized by applying quantum commutation rule [bφ, bp] = i~

Coulomb blockade and charge qubit When the area of junction is small, Fig.2.2 (a)., tunneling rate is small so EJ is small and capacitance is also small enough so that charging energy of a

Cooper pair in the Junction capacitor dominates the Hamiltonian, Ec = 1 2 (2e) 2 CJ EJ. This means it costs too much energy for a Cooper pair to tunnel across the junction.

Hamiltonian, operators:

The quantized Hamiltonian becomes H = EcNb + EJ(1 − cosbφ)

inductive energy now becomes a small term and the total energy mainly depends on charge energy, we move to number representation, where bφ = i · Nb, and use take {|ni}

Large junction and phase qubit For a junction with large area and thin barrier, critical current is large and capacitance is large as well. Consequently, EJ Ec. In this case, n is not a good quantum number any more formulas.

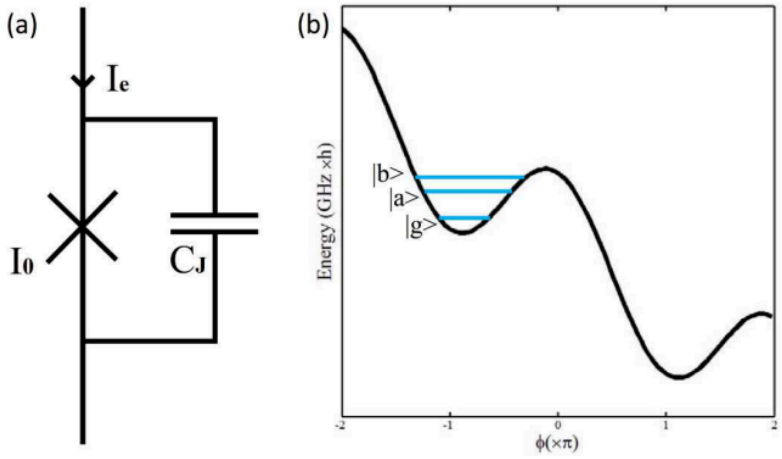

Figure 2.3: (a) Schematic circuit of DC current biased Phase Qubit. Cross stands for Josephson nonlinear inductor. (b) Washboard-like potential energy diagram of Phase Qubit. By adjusting Ie one can engineer each local potential well to include only three levels |gi, |ai, |bi.

With external field biased at φe = 1 2 φ0, we obtain a double-well potential (dashed line) giving rise to two degenerate ground state |le f ti for clockwise supercurrent and |right for counter-clockwise supercurrent, corresponding to magnetic flux in the loop going down and up. Because of the finite barrier between the two wells, the degeneracy is lifted due to the overlap of ground state wavefunction. So at the sweet point the two actual lowest states are (|↑i = |left to + |right |↓i = |left to − |right

Figure 2.4: (a) A big superconductor loop (blue) embedded with a Josephson junction (orange). Magnetic flux Φe goes through the loop to adjust the phase difference across the junction. (b) Schematic circuit of one-junction SQUID. The superconductor loop is treated as an inductor that is connected with the Josephson junction in series. (c) Potential energy diagram of the one

junction SQUID. When Φe = π, it forms two degenerate double well systems that can be used as a Flux Qubit. (d) Tunable dc SQUID.

2.4

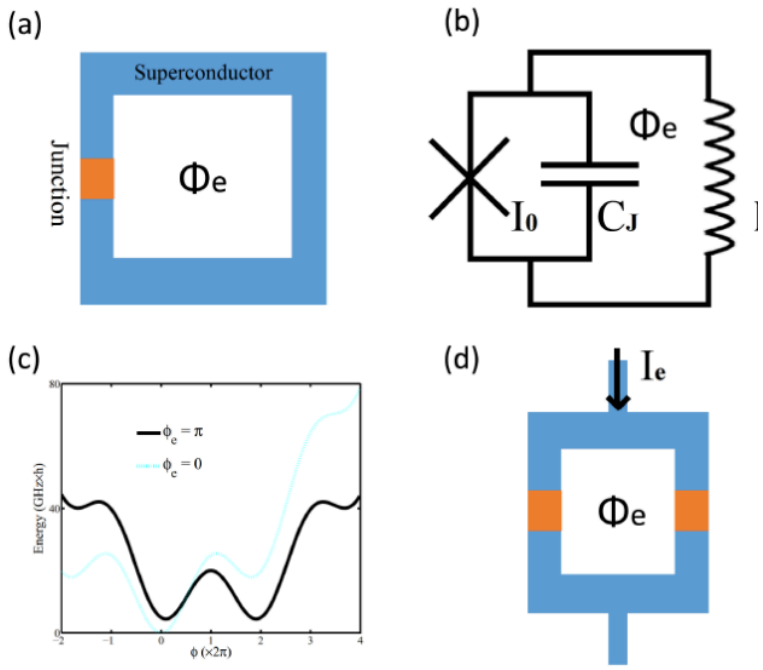

Charge qubit: We replace the single junction in the two junctions in the small junction limit Ec EJ. Similar to the derivation in dc-SQUID, we just need to replace the Josephson energy in Eq.(2.13) with a tunable term 2EJ cos φe 2 , and get the Hamiltonian H = Ec 2 (|1i h1| − |0i h0|) − EJ 2 (|0i h1| + |1i h0|)

With these two flux states one can build a qubit, the so-called ”flux qubit”. And this loop structure is sometimes called rf-SQUID. However, in real experiments, people usually shunt two large junctions and one small junction along the superconducting loop. [20] But the ground states have the same physical meaning. dc-SQUID: When there are two JJs along the loop, Fig.2.4(d), one needs two variables φ1 and φ2 as the phase difference across the two JJs. The superconducting loop now comes back to the form shown in Eq.(1.24). Coming with screening effect (2.18) one gets φ1 + φ2 = 2nπ − φe.

Electric fields: The scalar (electric) AB effect is less known than the vector (magnetic) version of the AB effect since it is harder to achieve the situation required for the electric AB effect where fields are vanishing while the potentials are non-zero. If one considers the fields and potentials for the cylindrical Faraday cage used in Aharonov and Bohm’s original paper, then the electron will invariably pass through some region with a non-zero electric field, although the field may be extremely small. To have the electron pass only through regions where there is no field, one needs to switch the fields and potentials on and off completely, i.e., it is necessary to

consider the time-dependent fields and potentials described by equation (2.23), where V(t) is a function with compact support. The existence of the scalar AB effect has been questioned (see for example the paper by Walstad [22]) exactly on the basis that some experimental confirmations of the effect [23] have the interfering electron passing through regions where the electric field is non-zero, and thus (potentially) one could explain the shift in an interference pattern in terms of classical forces rather than as a quantum phase effect.

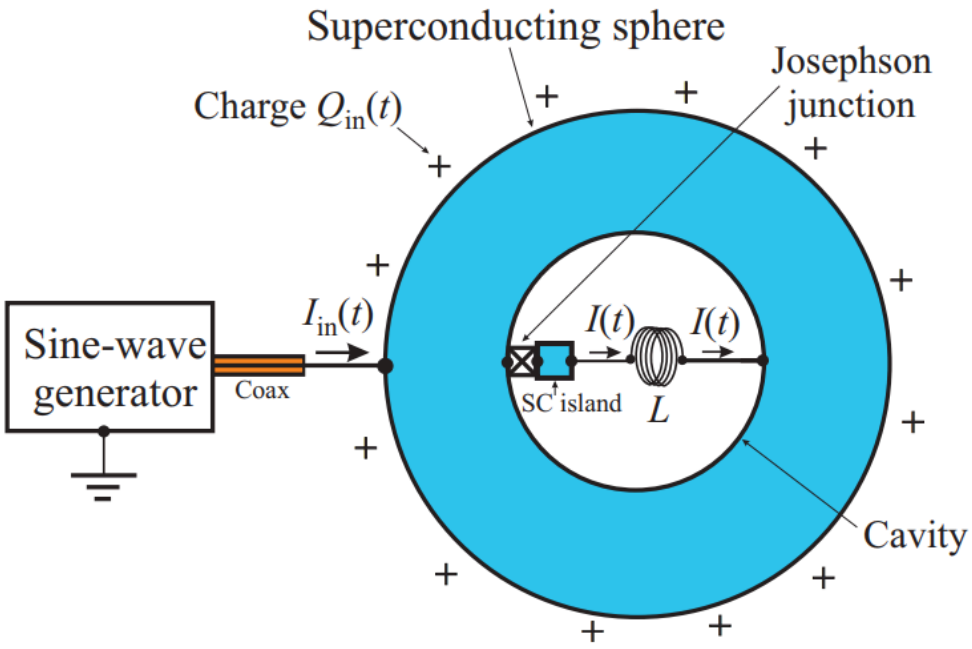

Figure 2.5: In the spherical superconducting (SC) shell, the SC artificial atom is formed with the hollow cavity and a superconducting wire on the horizontal axis. A SC island is connected to the cavity with a SC wire on one end and via a large Josephson junction on the other end. The effective inductance between the wire and cavity can be enhanced by increasing the number of switchbacks depicted as a solenoid. The spherical SC shell is made thick enough to prevent magnetic flux penetration into the interior.

potential V1 = V0 sinωt. For a superconductor subject to a voltage V (t), a phase factor φ(t) develops within the order parameter of the Cooper pair condensate, $\Psi = \sqrt{\rho} e^{i\varphi}$. The order parameter propagation to the interior gets retarded due to the junction. Hence a phase difference arises between the superconducting banks of the Josephson junction. This time-dependent difference drives a supercurrent according to the inverse AC Josephson effect.

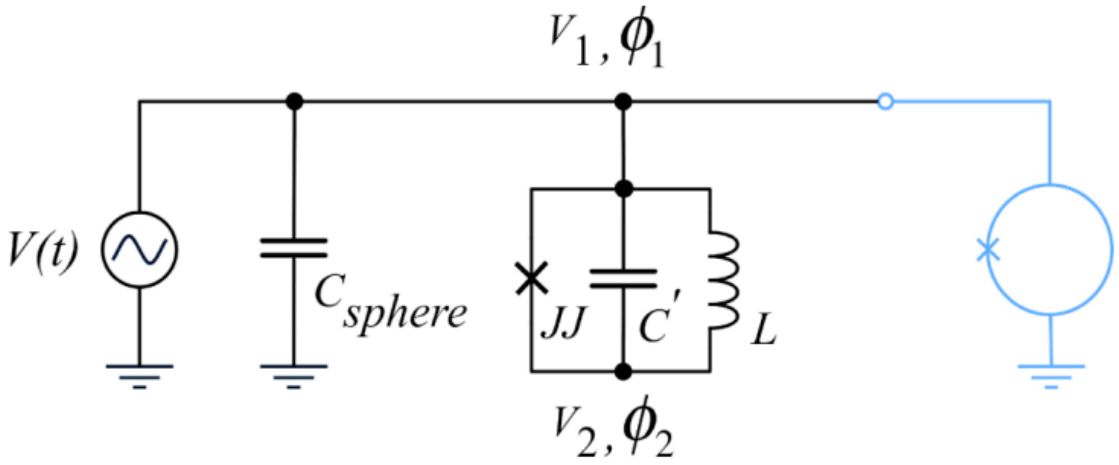

Figure 2.6: A simplified circuit includes three circuit loops that are connected on node 1. In the leftmost loop, a signal generator drives the system. The next loop with the capacitor Csph represents the spherical SC shell. C 0 and L are the effective capacitance and inductance of the SC island, respectively. The superconducting phase ϕ2 on the central superconductor (node 2) and ϕ1 on the sphere (node 1) are separated by a Josephson junction modeled with nonlinear inductance LJ and effective capacitance CJ. The right loop demonstrates a simple example of measurement, an rf-SQUID (light blue), although many possible variations of external lownoise readout exist to detect the change of ϕ1 in time.

Supernova and circuits: Nevertheless, there exist astrophysical situations, such as in the case of an exploding mass shell of a supernova, where the radius r0 (t) is the time-dependent quantity rather than the mass M (t). Then the gravitational AB phase shift may be large enough to be seen in practice. In any case, although the gravitational scalar potential may vary with time, nevertheless it must be independent of the position of the field point within the interior of the mass shell. This follows from Gauss's theorem. Therefore the atom within the mass shell experiences no classical forces. However, it can experience a nonzero quantum phase shift arising from the gravitational AB effect. The rest mass of the excited state of an atom or of a nucleus will be larger than the rest mass of the ground state of this atom or nucleus. This follows from Einstein's equation E = mc2 (2.29) In quantum mechanics, Einstein's equation becomes mc2 = hψ (t)| i~ ∂ ∂t |ψ (t)i (2.30) Thus the rest mass m in relativity is the expectation value of the energy operator i~∂/∂t in quantum mechanics. For example, when an atom is in a stationary state |ψ (t)i = |ΨEi exp (−iEt/~), it follows from (2.30) that mc2 = E hΨE |ΨEi =

The idea is to bring powerful processors such as i9 or powerful cores closer together, and imitate quantum behaviors for particle acceleration in circuits with superconducting materials. It is an idea that combines classical technical bases in FPGA design, for example, in conjunction with acceleration and masses that we can find in the universe. That is, at some point, the materials available on our planet become limited in order to build new engineering systems with data processing far superior to what is known. These ideas serve as a reference for the future construction of quantum circuits that imitate the efficiency of quantum algorithms in materials that could be found in other galaxies or stars.

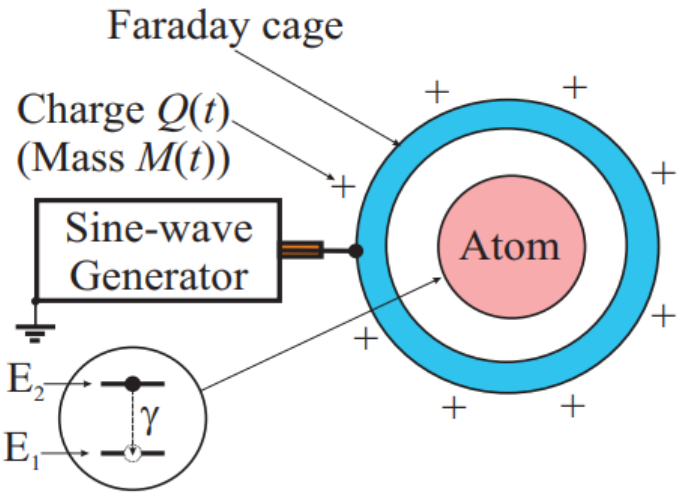

Figure 2.9: Two-level atom inside a spherical mass shell with a time-dependent mass M(t) that arises from a time-dependent charge Q(t). The mass M(t) results in a time-dependent gravitational redshift that leads to observable FM sidebands in the spectrum of the atom.

Quantum gravity or reverse or parallel gravity is also a reference and a way of understanding how by building another type of gravity we could manipulate photons or particle structures or laser equations.

Now from the expression for the gravitational AB phase (2.27), we expect that the atom in a stationary state with an energy E inside the mass shell will pick up an AB phase factor, so that |ψ (t)i = |ΨEi exp (−iEt/~) exp (−iϕ (t))

Waves: scalar AB effect experiment is Ψ = ΨpΨ s = e iΔEt/~Ψ p e −iΔEt/~Ψ s = ΨpΨ s

Circuit-Gates: Controlled quantum logic gates Two-qubit gates on the encoded qubits can be achieved by connecting the circuits of the encoded qubits as is shown in Fig. 2.14a. We consider two encoded qubits and use σα j as the Pauli operators for the first encoded qubit and τα j as Pauli operators for the second encoded qubit. Assume that the lower physical qubits in each

encoded qubit are connected with the coupling Hamiltonian Hcgate = −2λc cos(2(Em1 − Em2)t/~)σz2τz2.

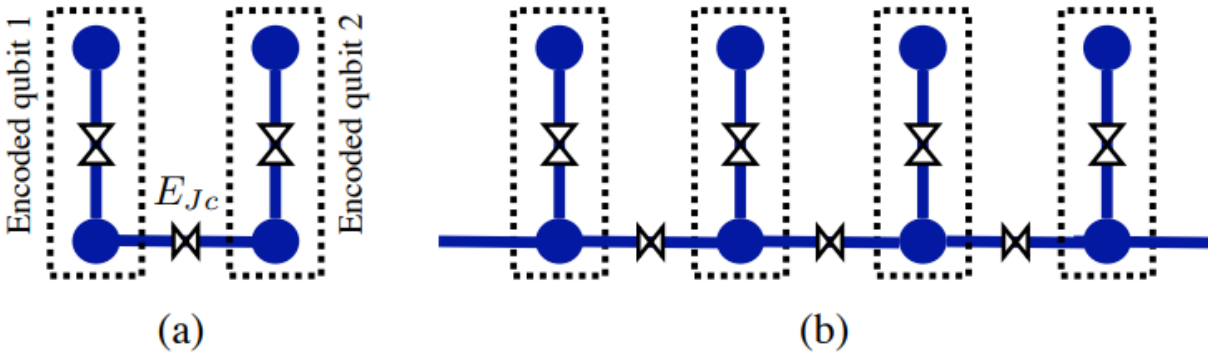

Gates and capacitive circuit components across the Josephson energy EJc and capacitive energy Ecc, we have Hcgate = − EJc 4 (σz2τz2 + σy2τy2) + Eccσx2τx2,

The coupling includes the extra terms σy2τy2 and σx2τx2, which only contain off-resonant leakage terms such as |1iσh3| ⊗ |3iτh1|. Under the time-dependent modulation cos(ωdt)

Thermalization-temperature: The concepts of state preparation and detection To implement the above quantum logic gates, we need to prepare the initial state of the system in the encoded subspace. This can be achieved by letting the coupled qubits relax to their ground states |1i via thermalization. Then, an ac driving Hprep = 2λp cos[(E1 − Em)t/~]σx1

Introduction of superconducting circuit quantum electrical dynamics:

In atomic quantum information devices, manipulation on qubit state can be enhanced by placing atoms into a cavity and hence coupled to coherent light. The dynamics is modeled as cavity quantum electrodynamics (CQED). Consider the qubit on a superconducting chip as an artificial ”atom”, AC signals propagating in the circuits as light. By coupling a superconducting qubit either capacitively or inductively to superconducting resonators, scientists have implemented the CQED method to manipulate quantum information on superconducting chips. Circuit QED is the formal terminology as the on-chip analogue of cavity QED. A key difference is that in circuit QED, the ‘atom’ does not move inside the ”cavity”, so the ‘atom’–field interaction has time to act without losing the ‘atom’ and a trapping system is not needed.

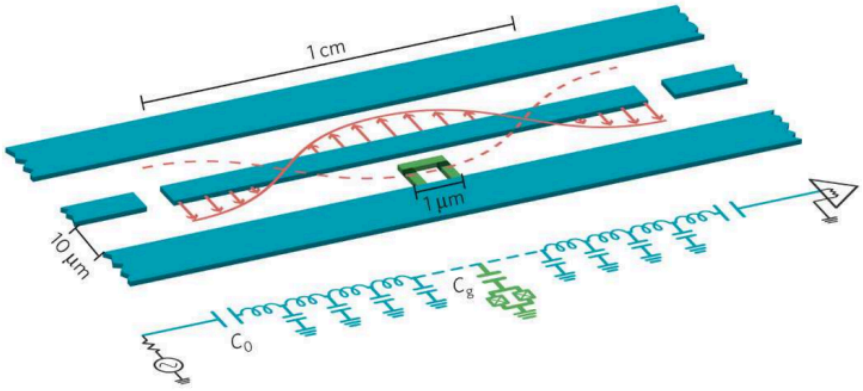

Figure 3.1: The upper part of the panel depicts a microstrip cavity (blue) that contains a charge qubit (green) placed at an antinode of the electric field. The microstripline can be used as a quantum bus. The lower part depicts this circuit in a lumped circuit representation. (Figure from Ref. [19]) C0 is the capacitance of the coupling capacitor to the measurement electronics, and Cg is the capacitance of the coupling capacitor to the charge qubit.

Neglecting rapidly oscillating terms, Hamiltonian further reduces to H = ~ω r (a † a + 1 2) + ~ω q 2 σ z + ~g(a †σ − + aσ +)

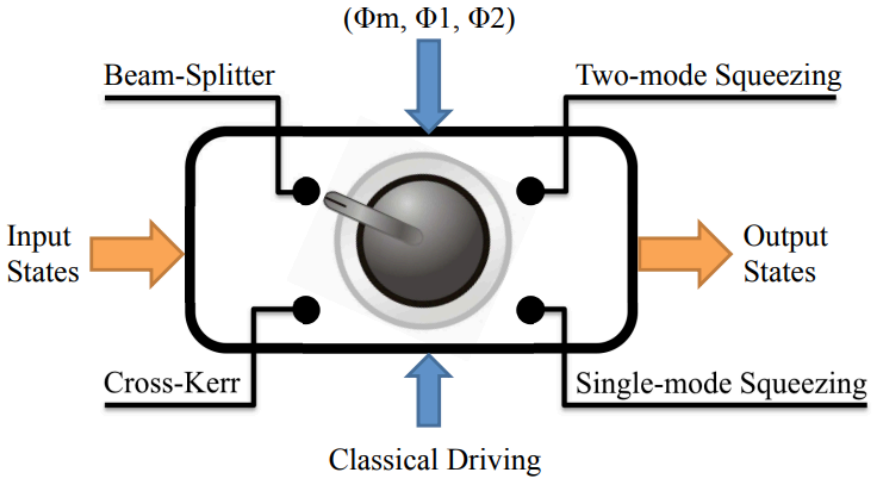

Figure 3.2: Illustration of dispersive FWM toolbox with controllable parameters Φm, Φ1, Φ2

Circuit operations: Implementing quantum operations on superconducting resonators is crucial for realizing quantum information protocols in such devices. A basic set of quantum operations for both the discrete-state and the continuous variable quantum information protocols on the resonator modes include the Bogoliubov-linear operations such as the beam-splitter operation.

Circuit

The central element of the toolbox is a quantum four-level system that couples with the superconducting resonators and can be constructed in many ways. For the discussion in this paper, we will consider a circuit for the toolbox that is made of two superconducting qubits coupling with each other. The Hamiltonian for the total system has the form Htot = Hq + Hr + Hp, (3.4) which includes the Hamiltonian for the four-level system Hq = P j Ej | jihj| with eigenstates | ji and eigenenergies Ej (j = a, b, c, d), the Hamiltonian for the resonators and their couplings to the qubits Hr = X i ~ωai aˆ † i aˆi + ~giσxi(ˆa † i + aˆi)

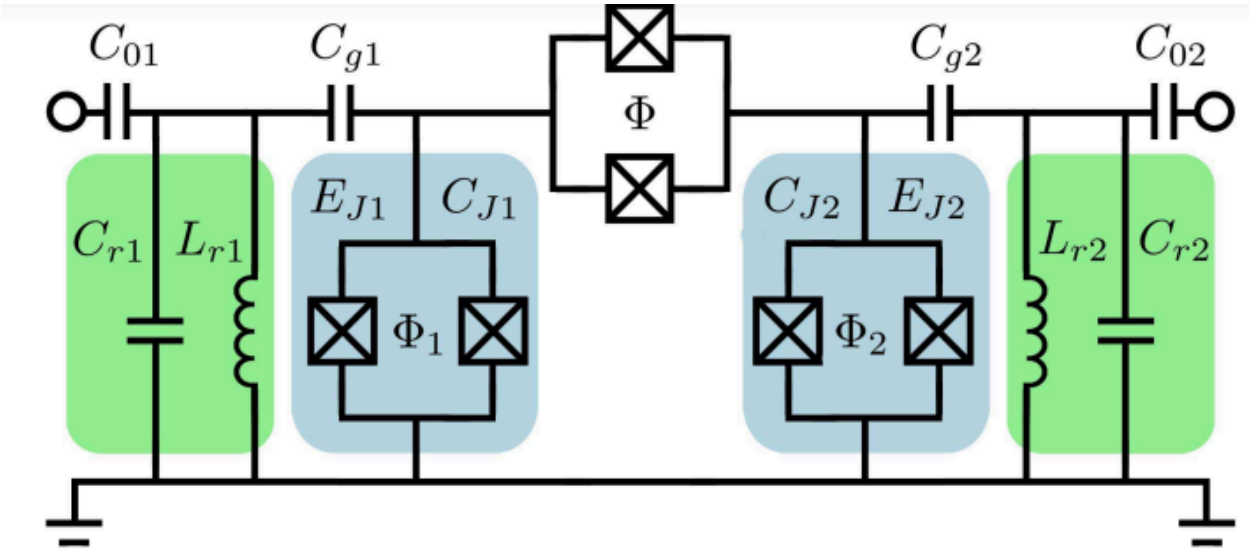

Core-Processor:

The latest Intel i9 processor is the **Intel Core i9-14900K**, part of the 14th generation Raptor Lake Refresh lineup. It features **24 cores (8 performance and 16 efficiency)**, supports speeds up to **6.0 GHz**, and has a **TDP of 125W**, which can boost to **253W** under heavy loads. This processor excels in multi-threaded tasks like physics simulations, making it suitable for laser operations and particle acceleration. However, depending on your project, earlier models like the **i9-13900K** might also provide adequate power at a lower cost.

The key specifications for the **Intel Core i9-14900K**, which is the most recent Intel i9 processor and well-suited for tasks like lasers or quantum computing:

1. **Cores and Threads**: 24 cores (8 performance + 16 efficiency), 32 threads.
2. **Base/Boost Frequency**: 3.2 GHz base, up to 6.0 GHz boost.
3. **TDP**: 125W, up to 253W.
4. **Architecture**: Raptor Lake Refresh.
5. **Memory Support**: DDR5 and DDR4.
6. **L3 Cache**: 36MB.

7. **Integrated Graphics**: Intel UHD 770.

It is optimized for multi-threaded tasks and high computational loads.

Qubits figures, academic research:

qubits can be controlled by external electromagnetic fields such as the magnetic flux in the loop of a superconducting quantum interference device (SQUID) and the bias voltage on a superconducting island, depending on specific circuit design. Different coupling mechanisms between superconducting qubits have also been studied, such as capacitive coupling, Josephson coupling, and inductive coupling. [109–113] Decoherence in superconducting qubits has improved greatly in the past few years with T ? 2 exceeding 95 µsec. recently observed. [59, 114–116] To illustrate our scheme, we study a toolbox made of two superconducting charge qubits. [18] We want to emphasize, however, the FWM approach studied here is a general scheme that can be applied to other superconducting qubits with different forms of coupling. As shown in Fig. 3.3, the charge qubits couple with each other via a tunable Josephson junction and a capacitor where the effective Josephson energy EJm can be adjusted by varying the magnetic flux Φ in the loop.

The Josephson energies EJi of the qubit junctions can be adjusted by changing the magnetic flux Φ1,2 in the qubit loops. The Hamiltonian for the coupled qubits can be derived using a Lagrangian approach with Hq = (EJ1/2)σz1 + (EJ2/2)σz2 + Hint (3.6) Hint = Emx σx1σx2 + b0σy1σy2 + b0σz1σz2 (3.7) where Emx is the capacitive coupling due to capacitance Cm and b0 = EJm/4Emx is the ratio between the Josephson coupling and the capacitive coupling. Here, we assume the qubits are biased to have zero charging energy so that the qubit energies are the Josephson energies EJi. [117]

We define the total capacitance connected to the superconducting island of the ith qubit as CΣi = CJi+Cgi+Cm and the total capacitance connected to the ith resonator as CΣri = Cri+Cgi+ C0i , where Cgi is the capacitance that couples a resonator to its corresponding qubit, CJi is the Josephson capacitance, Cri is the resonator capacitance, and C0i is the capacitance that couples 57 to external circuit, as labeled in Fig. 3.3. With the capacitances satisfying CΣri CΣi Cm, the capacitive coupling Emx can be derived as Emx ≈ Cme 2 / h CΣ1CΣ2 − C 2 m i . (3.8)

The eigenenergies of the Hamiltonian Hq are Ea = Emxb0 − Es+/2, (3.9a) Eb = −Emxb0 − Es−/2, (3.9b) Ec = −Emxb0 + Es−/2, (3.9c) Ed = Emxb0 + Es+/2, (3.9d) where Es± = p (EJ1 ± EJ2) 2 + 4E 2 mx(1 ∓ b0) 2

The models can be adjusted by varying the qubit energies EJi and the Josephson coupling EJm. The eigenstates are |ai = − sin θ+ |0102i + cos θ+ |1112i, (3.10a) |bi = cos θ− |0112i − sin θ− |1102i, (3.10b) |ci = sin θ− |0112i + cos θ− |1102i, (3.10c) |di = cos θ+ |0102i + sin θ+ |1112i, (3.10d) where |0ii and |1ii are the single-qubit eigenstates in the σzi basis and sin θ± = p [Es± ± (EJ1 ± EJ2)] /2Es±.

Intel core 9:

Architecture:

1. **Intel i9 for high-performance tasks** (quantum calculations, simulations).
2. **Zephyr RTOS running on a microcontroller** (manages real-time tasks like laser control or communication).
3. **Interface via serial, SPI, or I2C** (Intel communicates with the microcontroller for real-time data processing).

Steps:

1. **Set up Zephyr RTOS** on your microcontroller with CMake and configure the real-time tasks.
2. **Develop C++ code** for communication and computation.

Example Zephyr RTOS Code (C++):

```
#include <zephyr.h>
#include <device.h>
#include <drivers/gpio.h>

#define LED_PIN DT_ALIAS_LED0_GPIOS_PIN
#define SLEEP_TIME_MS 1000

void main() {
    const struct device *dev;
    dev = device_get_binding(DT_ALIAS_LED0_GPIOS_CONTROLLER);
    gpio_pin_configure(dev, LED_PIN, GPIO_OUTPUT);

    while (1) {
        gpio_pin_set(dev, LED_PIN, 1);
        k_msleep(SLEEP_TIME_MS);
        gpio_pin_set(dev, LED_PIN, 0);
        k_msleep(SLEEP_TIME_MS);
    }
}
```